DOI: 10.1002/ejic.200800149

Influence of a Pyrazyl Linker on the Physicochemical Properties of Homodinuclear Bis(cyclen) and Bis(cyclam) Complexes

Sanae El Ghachtouli,[a] Cyril Cadiou,[a] Isabelle Déchamps-Olivier,[a] Françoise Chuburu,*[a] Michel Aplincourt,[a] Thierry Roisnel,[b] Véronique Turcry,[c] Véronique Patinec,[c] Michel Le Baccon,[c] and Henri Handel[c]

Keywords: Copper / Nickel / Bis(cyclen) ligands / Bis(cyclam) ligands / Electrochemistry

Cu^{II} and Ni^{II} complexes of bis(cyclen)pyrazine and bis(cyclam)pyrazine, $[Cu_2\mathbf{L^1}]^{4+}$, $[Ni_2\mathbf{L^1}]^{4+}$, $[Cu_2\mathbf{L^2}]^{4+}$, $[Ni_2\mathbf{L^2}]^{4+}$, have been isolated and characterised by UV/Vis and EPR spectroscopy. Complex $[Cu_2\mathbf{L^1}]^{4+}$ was characterised by X-ray diffraction. The crystallographic structure indicated that the two metal cations are held in a square-pyramidal geometry, the central nitrogen pyrazine atoms occupying the apical position of each metal centre. In solution, the EPR spectrum of $[Cu_2\mathbf{L^1}]^{4+}$ revealed the presence of two isomers, one of which was the previous crystallised complex. For $[Ni_2\mathbf{L^2}]^{4+}$, the electrochemical studies have highlighted the presence of two distinct geometries for the complex (type III and type V). From the electronic point of view, EPR and electrochemical measurements indicated that in these complexes the pyrazine bridge behaves as a poorly efficient exchange bridging ligand between the two metal centres.

Introduction

Tetraazamacrocyclic ligands like cyclen and cyclam, even when they are *N*-functionalised, are known to be good complexing agents towards first-row transition metals.[1] This is a reason why these ligands are used as constitutive subunits in more sophisticated ligands such as bistetraazamacrocycles,[2] macrotricycles[3] and trismacrocycles.[4] If their molecular structure is properly designed, in particular if besides metal ion coordination, noncovalent interactions are anticipated (hydrogen-bonding, hydrophobic or electrostatic interactions), they can be developed as artificial receptors, like anion receptors for instance. Bis- and trismacrocyclic Zn^{II} cyclen complexes developed by Kimura and co-workers have proved to be extremely efficient in binding mono- and diphosphate nucleotides in aqueous solution at physiological pH.[5] More fundamentally, bismacrocyclic ligands are interesting, because they are able to hold two metal centres in proximity, which can allow the possible development of metal–metal interactions and mimic the multinuclear metal arrays at the active sites of several metalloenzymes.[6] Nevertheless, these interactions, often termed "superexchange" because of the large distances between the metal ions involved, remain weak, and the bridging atoms between the metal ions determine the magnitude of the exchange interaction.[7] For this purpose and in order to tune the metal–metal distance in bismacrocyclic systems, the most straightforward structural parameter to modify is the linker between the two macrocyclic cavities. Kaden, Fabbrizzi and co-workers showed, through electrochemical and EPR studies of metallic bistetraazamacrocyclic complexes, that below an intermetallic distance of about 8 Å, these metal–metal interactions can be detected.[8] Recently, it was shown too that in pyridyl bis(cyclen) and bis(cyclam) complexes, the modification of the metal stereochemistry triggered by a metal-centred electron transfer[9] associated with the presence of coordinating supplementary atoms on the linker between the two macrocyclic cavities enhance these interactions.[10] In order to gain much insight into the specific influence of the bridging atoms between the metal ions, it seemed to us relevant to prepare bismacrocyclic copper(II) and nickel(II) complexes based upon cyclen and cyclam cavities joined by a pyrazine bridge (Scheme 1). This rigid spacer was recently used to evaluate the superexchange mechanism in pyrazine-bridged copper(II) complexes.[11] Our goal is to get a characterisation of the complexes both in the solid state and in solution, in order to analyse their electronic properties. In particular, we wish to evaluate, in bismacrocyclic complexes, the influence of the pyrazine bridge on the electronic exchange between the two metal ions.

[a] Université de Reims Champagne-Ardenne, Institut de Chimie Moléculaire de Reims, UMR CNRS 6229, Groupe de Chimie de Coordination,
B. P. 1039, 51687 Reims Cedex 2, France
[b] UMR CNRS 6511, Institut de Chimie de Rennes, CS 74205, 35042 Rennes Cedex, France
[c] UMR CNRS 6521, Université de Bretagne Occidentale, B. P. 809, 29285 Brest Cedex, France
E-mail: francoise.chuburu@univ-reims.fr
Supporting information for this article is available on the WWW under http://www.eurjic.org or from the author.

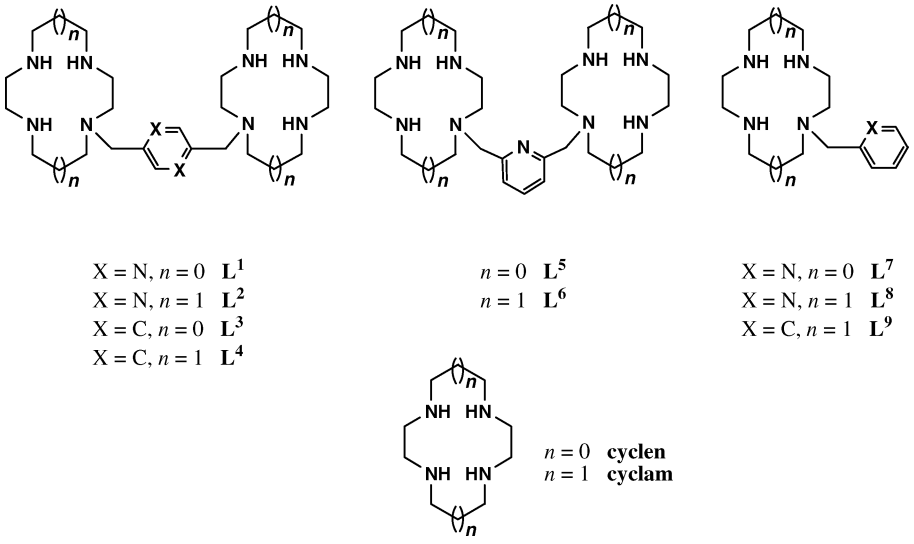

Scheme 1.

Results and Discussion

Ligands **L**[1] and **L**[2] were synthesised according the bis(aminal) methodology.[12] The protonation constants of the ligands and the overall formation constants of the copper complexes were determined by means of potentiometric titrations at 20 °C with I = 1 (KNO_3) (see Exp. Sect.).

Acid–Base Behaviour of L[1] and L[2]

The titration of the solutions of **L**[1] and **L**[2] gave rise to neutralisation curves with a single inflexion point at pH ≈ 7 for both ligands (Figure S1). The mathematical treatment of these data with PROTAF software[13] allowed the determination of the $\log K_{01h}$ values, which are gathered in Table 1 with those of relevant ligands like cyclen, cyclam and *para*-xylyl **L**[3] and **L**[4] bismacrocycles.[12] For **L**[1] and **L**[2], the five calculated protonation constants compare well with the constants previously determined for the relevant **L**[3] and **L**[4] ligands. For each bismacrocyclic ligand, the first two protonation constants have to be compared with the first protonation constant of the sole cavity (of cyclen or cyclam, as appropriate). The similarity between the values indicates that in bismacrocyclic ligands the two first protons are added alternatively in the two cavities. This can be easily understood in terms of minimisation of electrostatic repulsion between positive charges in the protonated species.[14,15] These observations still hold for the third and fourth protonations. The question that should be raised concerns the constant value associated with the protonation of the pyrazine nitrogen atoms. The consideration of the protonation constants determined for aromatic nitrogen heterocycles shows that in methylamino-substituted heterocycles, this constant is lowered with substitution according to $\log K$ = 5.3 for pyridine, $\log K$ = 2.3 for 2-methylaminopyridine and $\log K < 1$ for 2,6-dimethylaminopyridine.[16] Moreover, the data available for the protonation of pyrazine nitrogen atoms[16] indicates that their affinity for protons is low, since they can only be protonated at a pH lower than 1.5. Therefore, for **L**[1] and **L**[2], it seems that the fifth protonation constant also corresponds to the addition of a proton to a macrocyclic cavity.

Table 1. Ligand protonation constants ($\log K_{01h}$) and overall formation constants ($\log \beta_{mlh}$) of the copper complexes: the numbers in parentheses refer to the estimated standard deviations for the last significant digit (95% confidence).

	L[1][a]	**L**[2][a]	**L**[3][b]	**L**[4][b]	Cyclen[c]	Cyclam[c,d]
$L + H^+ \rightleftharpoons LH^+$	10.7(2)	11.4(2)	11.1	12.3	10.97	11.58
$LH^+ + H^+ \rightleftharpoons LH_2^{2+}$	10.44(6)	11.07(6)	10.5	11.1	9.87	10.62
$LH_2^{2+} + H^+ \rightleftharpoons LH_3^{3+}$	9.60(5)	10.65(4)	9.44	9.8	<2	1.61
$LH_3^{3+} + H^+ \rightleftharpoons LH_4^{4+}$	8.71(2)	9.56(2)	8.75	8.9	<2	2.42
$LH_4^{4+} + H^+ \rightleftharpoons LH_5^{5+}$	1.9(1)	2.0(1)	<2	2.8		
$LH_5^{5+} + H^+ \rightleftharpoons LH_6^{6+}$	<2	<2	<2	1.7		
$2Cu^{2+} + L \rightleftharpoons Cu_2L^{4+}$	39.2(3)	41.9(2)	39.2	44.0		
$Cu^{2+} + L \rightleftharpoons CuL^{2+}$	20.0(3)	20.9(4)	19.6	23.5	23.3	26.5
$Cu^{2+} + L + H^+ \rightleftharpoons CuLH^{3+}$	30.0(3)	32.0(3)	30.4	33.8		
$Cu^{2+} + L + 2H^+ \rightleftharpoons CuLH_2^{4+}$	39.0(2)	42.2(2)	39.4	42.3		

[a] Potentiometric titrations carried out at 20.0(1) °C, I = 1 mol L^{-1}(KNO_3) (this work). [b] Ref.[14]. [c] Ref.[1]. [d] Ref.[34].

Thermodynamic Stability of Complexes $[Cu_2L^1]^{4+}$ and $[Cu_2L^2]^{4+}$

The complexation kinetics of the macrocycles cyclen and cyclam is known to be pH-dependent. In order to take into account this phenomenon, the copper complexation of **L¹** and **L²** was investigated according to the procedure of Soibinet and co-workers.[14] The solutions were prepared for several [total ligand]/[total metal] ratios (C_L/C_M) at acidic initial pH and stored under argon in a thermoregulated enclosure at 40 °C for four, six and eight weeks. These conditions are required, because the kinetic complexation is slow. Prior to potentiometric analysis, it was checked by EPR spectroscopy that, in these experimental conditions and for $C_L/C_M > 1$, mononuclear complexes were formed (four equidistant lines in the spectrum in the whole pH range; see Figures S2 and S3) while for $C_L/C_M < 1$, dinuclear complexes were formed (more than four lines in the spectrum in the whole pH range; see Figures S2 and S3).[14] The overall stability constants associated to the formation of all these complexes are gathered in Table 1. The logarithmic values of the overall constants are (20.0 ± 0.3) and (20.9 ± 0.4) for the mononuclear species $[CuL^1]^{2+}$ and $[CuL^2]^{2+}$, respectively, and (39.2 ± 0.3) and (41.9 ± 0.2) for the dinuclear complexes $[Cu_2L^1]^{4+}$ and $[Cu_2L^2]^{4+}$, respectively. These $\log\beta_{110}$ and $\log\beta_{210}$ values are similar to those determined for the relevant complexes $[Cu_mL^{3,4}]^{2m+}$ where $m = 1$ or 2[14] (for the corresponding species distribution diagrams see Figures S2 and S3). From these values, we deduce that the stepwise complexation constants ($\log K = \log\beta_{210} - \log\beta_{110}$) corresponding to the addition of a second metal ion to the mononuclear species are 19.2 and 21.0 for $[Cu_2L^1]^{4+}$ and $[Cu_2L^2]^{4+}$, respectively. These values are similar to the overall constants determined for the mononuclear species $[CuL^{1,2}]^{2+}$ and indicate that the addition of the second metal ion on $[CuL^{1,2}]^{2+}$ is not affected by the presence of the first one. Furthermore, the comparison of the overall stability constants for the bismacrocyclic ligands **L¹⁻⁴** suggests that, whatever the ligand structure, their affinity towards copper is similar. Since in this direct comparison, the differences in the basicities of the ligands are not taken into account, the concentration $[Cu^{2+}]_{free}$ was determined across the pH range (see Figure S4). The concentration of the free metal cation represents a direct indication of the ligand–metal affinity with consideration of all involved equilibria.[17] The weaker the free metal concentration, the higher the ligand metal affinity. Actually, the corresponding plots indicated that the complexing ability of **L¹** is the same as that of its homologue **L³**, while the complexation ability of **L²** is weaker than that of **L⁴**. This suggests that, in solution, the pyrazine bridge coordination is weak and does not counterbalance the poor σ-donor ability of tertiary amines relative to secondary amines.[18] So, in order to have a better insight of the structures of the dinuclear complexes, a study of the complexes in the solid state was undertaken.

Molecular Structure of Complexes $[Cu_2L^1]^{4+}$ and $[Ni_2L^1]^{4+}$

To provide a proof of the stoichiometry and the structure of the complexes, a crystallographic study was carried out. Single crystals suitable for X-ray analysis were obtained only with **L¹**. For the $[Cu_2L^1]^{4+}$ complex, the single crystals were isolated by slow diffusion of ethyl ether into an acetonitrile solution of the complex. A Schakal depiction of $[Cu_2L^1]^{4+}$ is provided in Figure 1. The structure is centrosymmetrical, and the two copper ions are pentacoordinate in a square-pyramidal geometry as expected for copper held in a cyclen cavity. Each metal ion is coordinated by the four macrocyclic nitrogen atoms of each macrocycle and in an apical position by a nitrogen atom of the pyrazine bridge. Selected bond lengths and angles are given in Table 2. The Cu–NH bond lengths [2.000(4)–2.018(3) Å] are close to the ones in the bis(*para*-xylylcyclen) copper complex,[14] while the bonds to the tertiary macrocyclic nitrogen atoms are slightly longer [2.047(3) Å]. This is generally attributed to the consequence of the *N*-alkylation on these atoms.[19] The bond to the nitrogen atom of the pyrazine ring is longer {*d*[Cu–N(5)] = 2.159(3) Å}. The coordination of the linker N(5) atom allows the formation of an efficient five-membered chelate ring, which leads to a smaller N(5)–Cu–N(3) angle of 81.6(2)° for the N(3) nitrogen carrying the pyrazine linker [relative to values of 96.7(2) to 126.7(2)° for the other three N(5)–Cu–N angles]. These values agree with a square-pyramidal geometry (Addison parameter,[20] $\tau = 0.01$). The distance of each copper ion with regard to its corresponding macrocyclic cavity is about 0.53 Å. At last, for this complex, the intramolecular Cu–Cu distance is measured to be 7.025 Å. This distance is intermediate between those determined in homologous complexes with a *para*-xylyl bridge (11.539 Å)[14] and a pyridine linker (5.779 Å in $[Cu_2L^5]^{4+}$).[10]

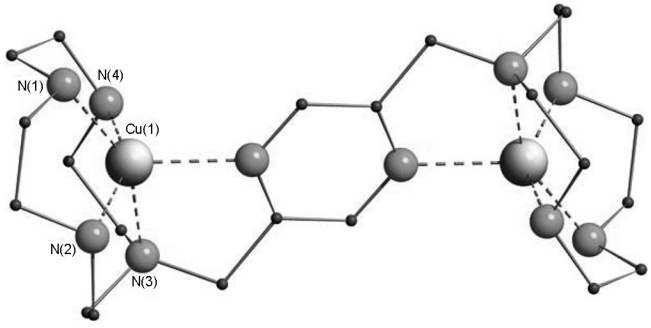

Figure 1. Schakal diagram of $[Cu_2L^1]^{4+}$.

Table 2. Selected bond lengths (in Å) and angles (in °) for $[Cu_2L^1]^{4+}$.

Cu(1)–N(1)	2.000(4)	Cu(1)–N(4)	2.012(3)
Cu(1)–N(2)	2.018(3)	Cu(1)–N(5)	2.159(3)
Cu(1)–N(3)	2.047(3)		
N(1)–Cu(1)–N(2)	85.92(16)	N(2)–Cu(1)–N(5)	113.16(13)
N(1)–Cu(1)–N(3)	151.25(13)	N(3)–Cu(1)–N(5)	81.62(11)
N(1)–Cu(1)–N(4)	85.31(16)	N(4)–Cu(1)–N(2)	147.90(14)
N(1)–Cu(1)–N(5)	126.69(13)	N(4)–Cu(1)–N(3)	86.38(13)
N(2)–Cu(1)–N(3)	86.64(14)	N(4)–Cu(1)–N(5)	96.72(13)

For $[Ni_2L^1]^{4+}$ and $[Cu_2L^2]^{4+}$, we failed to obtain single crystals suitable for a good X-ray structure determination. Nevertheless, for these complexes the crystallisation

attempts allowed us to elucidate the metal coordination spheres (see Figures S5 and S6). For $[Ni_2\mathbf{L^1}]^{4+}$ (Figure S5), the two nickel ions are octahedral: the pyrazine nitrogen atoms N(5) are coordinated to each metal centre, and the sixth position is occupied by a solvent molecule. For $[Cu_2\mathbf{L^2}]^{4+}$ (Figure S6), the two copper ions are held in a pentacoordinate environment constituted by the four macrocyclic nitrogen atoms and by a pyrazine nitrogen atom. The intermetallic M^{II}–M^{II} distances are estimated at 6.9 Å for $[Ni_2\mathbf{L^1}]^{4+}$ and 7.2 Å for $[Cu_2\mathbf{L^2}]^{4+}$. For $[Cu_2\mathbf{L^2}]^{4+}$ this distance is smaller than the one estimated in the homologous *para*-xylyl complex by EPR measurements ($d > 9.6$ Å).[21]

All these structures show that the pyrazine nitrogen atoms are coordinated to the metal centres. Furthermore, the presence of two coordinating nitrogen atoms on the intermacrocyclic spacer seems to induce both the existence of a symmetry element through the spacer and a shortening of the intermetallic distance.

Electronic Absorption Spectroscopy of Complexes $[Cu_2L^{1,2}]^{4+}$ and $[Ni_2L^{1,2}]^{4+}$

The absorption maxima of complexes $[Cu_2\mathbf{L^{1,2}}]^{4+}$ and $[Ni_2\mathbf{L^{1,2}}]^{4+}$ in water and in acetonitrile are listed in Table 3. The comparison of these data with those obtained in solid state for the same complexes is a good indication of the nature of the metal coordination sphere in solution.

Table 3. Electronic absorption data [λ /nm (ε /mol^{-1} L cm^{-1})] for complexes $[Cu_2\mathbf{L^{1,2}}]^{4+}$, $[Ni_2\mathbf{L^{1,2}}]^{4+}$ and $[Cu\mathbf{L^{7,8}}]^{2+}$.

Complex	In H_2O	In CH_3CN	Solid
$[Cu_2\mathbf{L^1}]^{4+}$	568 (222)	575 (222)	570
$[Cu_2\mathbf{L^2}]^{4+}$	556 (202)	551 (210)	540
$[Ni_2\mathbf{L^1}]^{4+}$	848 (41), 529 (150)	839 (43), 530 (152)	809, 532
$[Ni_2\mathbf{L^2}]^{4+}$	840 (37), 527 (148)	840 (38), 530 (149)	800, 532
$[Cu\mathbf{L^7}]^{2+}$[a]	595 (218)	601 (247)	600
$[Cu\mathbf{L^8}]^{2+}$[a]	541 (228)	550 (125)	551

[a] Ref.[18].

Copper Complexes

For $[Cu_2\mathbf{L^1}]^{4+}$, in water, the visible spectrum exhibits a broad band with a maximum at 568 nm. The position of this band, associated to the copper d→d* transition, is poorly affected by the nature of the solvent and is similar in the solid state and in solution. This means that the copper environment is maintained on going from the solid state to the solution. Furthermore, this λ_{max} value compares well with the one determined for the reference complex $[Cu\mathbf{L^5}]^{2+}$,[18] which is typical of a pentacoordinate copper ion. So, for $[Cu_2\mathbf{L^1}]^{4+}$ in solution, the pyrazine nitrogen atoms remain coordinated to the copper ions in a CuN_5 chromophore. For $[Cu_2\mathbf{L^2}]^{4+}$, the spectral characteristics are similar regardless of the recording conditions. The λ_{max} value (λ_{max} = 556 nm in H_2O) compares well with the one determined for $[Cu\mathbf{L^6}]^{2+}$[18] (λ_{max} = 541 nm), where the copper coordination sphere is constituted by the four macrocyclic nitrogen atoms and the nitrogen atom of the pyridine linker. This value also indicates that the configuration of the macrocyclic cavity is of type III according to Bosnich nomenclature.[22] So, for $[Cu_2\mathbf{L^2}]^{4+}$ in solution, the pyrazine nitrogen atoms are coordinated to the copper ions in a CuN_5 chromophore.

Nickel Complexes

The visible spectra of the nickel complexes $[Ni_2\mathbf{L^{1,2}}]^{4+}$ can be interpreted on the basis of an octahedral coordination of the metal. Whatever the conditions, two bands are observed for both complexes corresponding to the predicted $^3A_{2g}\rightarrow{}^3T_{2g}$ (950–800 nm) and $^3A_{2g}\rightarrow{}^3T_{1g}$ (F) (560–500 nm) transitions for a d^8 metal ion under octahedral symmetry, the third transition $^3A_{2g}\rightarrow{}^3T_{1g}$ (P) (300–400 nm) being hidden by the strong absorbance of the ligand. For each complex, λ_{max} values determined on going from the solid state to solution are similar, which indicates that the nickel environment is maintained in solution. This suggests that the pyrazine nitrogen atoms are coordinated to the nickel centres.

Electrochemical Properties of the Bismacrocyclic Complexes

Since the presence of two coordinating nitrogen atoms on the intermacrocyclic spacer involves a decrease in the intermetallic distance, it is important to check whether this influences the interaction between the two metal centres, in particular when the metal redox state is modified. For this purpose, the redox behaviour of the binuclear complexes was investigated by electrochemistry. Since the mono-*N*-functionalised cyclen cavity is not well adapted to stabilise +I and +III oxidation states for copper and nickel,[23] only the binuclear $[Cu_2\mathbf{L^2}]^{4+}$ and $[Ni_2\mathbf{L^2}]^{4+}$ complexes were investigated by cyclic voltammetry in CH_3CN, with a glassy carbon disk as the working electrode and the Fc^+/Fc couple as reference.

The $[Cu_2\mathbf{L^2}]^{4+}$ complex exhibits two irreversible systems separated by approximately 2.50 V. The Cu^{II}–Cu^{I} cathode peak is measured at –1.25 V vs. Fc^+/Fc, while the anode Cu^{II}–Cu^{III} peak appears at 1.27 V vs. Fc^+/Fc. These values are in agreement with those already measured for copper–cyclam complexes.[10,24] Moreover, the high anode current detected for the first cycle and the decrease in its intensity with the number of cycles suggest that the Cu^{III} species is unstable in these conditions and reacts rapidly in the medium.

The redox behaviour of $[Ni_2\mathbf{L^2}]^{4+}$ was investigated in similar conditions. In reduction, only one quasireversible Ni^{II}–Ni^{I} system at –1.35 V vs. Fc^+/Fc (ΔE_p = 130 mV) is observed. In oxidation (Figure 2), the voltammogram presents two quasireversible waves. The oxidation half potentials of these systems are at 0.80 V vs. Fc^+/Fc (ΔE_p = 120 mV) and 1.16 V vs. Fc^+/Fc (ΔE_p = 120 mV). Relative to the known $E^{ox}_{1/2}$[Ni(cyclam)]$^{2+}$ potential (0.64 V vs.

Fc^+/Fc), these potentials are shifted to higher values. This is generally attributed to the reduction of the in-plane metal–ligand interaction under the influence of the macrocyclic *N*-substitution.[25] In order to explain the existence of two Ni^{II}–Ni^{III} oxidation systems for $[Ni_2\mathbf{L^2}]^{4+}$, two hypotheses can be formulated. The first one implies the existence of interactions between the two metal centres. In this case, the oxidation of the first Ni^{II} would make more difficult the oxidation of the second one, leading to two separate systems. This mixed-valence behaviour has previously been observed with a dinuclear Ni^{II} complex of ligand $\mathbf{L^6}$.[10] If $[Ni_2\mathbf{L^2}]^{4+}$ presents such a behaviour, its two Ni^{II}–Ni^{III} systems must be similar, i.e. they must present the same shape and current intensities. The second hypothesis implies the existence of isomers for $[Ni_2\mathbf{L^2}]^{4+}$ in solution, which is in agreement with the isolation of two $[Ni_2\mathbf{L^2}]^{4+}$ samples during the synthesis of the complex (see Exp. Sect.). During the electrochemical study of the $[Ni_2\mathbf{L^2}]^{4+}$ samples (for which the purity was checked by mass spectrometry and elemental analysis), two voltammograms were recorded (Figure 2): the voltammogram of the first sample (Figure 2a) shows that the currents for the second oxidation system are higher than those for the first system, while for the second sample (Figure 2b), the first oxidation system predominates. This tends to prove that the two Ni^{II}–Ni^{III} systems are not due to a mixed-valence behaviour for one species but rather to the existence of two isomers of $[Ni_2\mathbf{L^2}]^{4+}$. This is supported by the fact that cyclam complexes are known to exist as several isomers in solution.[8–10,22] The identification of the isomers can be taken further by comparison of the $E^{ox}_{1/2}$ values of relevant complexes for which the stereochemistry was elucidated (Table 4). The comparison of the $[Ni_2\mathbf{L^2}]^{4+}$ $E^{ox}_{1/2}$ values with those of $[Ni\mathbf{L^8}]^{2+}$ and $[Ni\mathbf{L^9}]^{2+}$[26] indicates that, for $[Ni_2\mathbf{L^2}]^{4+}$, the first oxidation system at 0.80 V can be ascribed to the oxidation of two nickel ions fitted in type III cyclam cavities, while the second one corresponds to the oxidation of two nickel ions held in type V cyclam cavities. Moreover, no modification in the intensity or reversibility of the waves can be observed in the cycle, which means that at the voltammetry time scale, the interconversion between these isomers is very slow or even prevented. Relative to $[Ni_2\mathbf{L^6}]^{4+}$,[10] the electrochemical study of $[Ni_2\mathbf{L^2}]^{4+}$ shows no mixed-valence behaviour, which means that, unlike the pyridine bridge, the pyrazine bridge does not improve metal–metal interactions. Previous work concerning the superexchange mechanism in dinuclear, pyrazine-bridged copper(II) complexes have already established that pyrazine and pyrazine derivatives are relatively inefficient exchange bridging ligands.[11a,11b,11c,11e] In order to understand the nature of the weak superexchange interaction in the pyr-

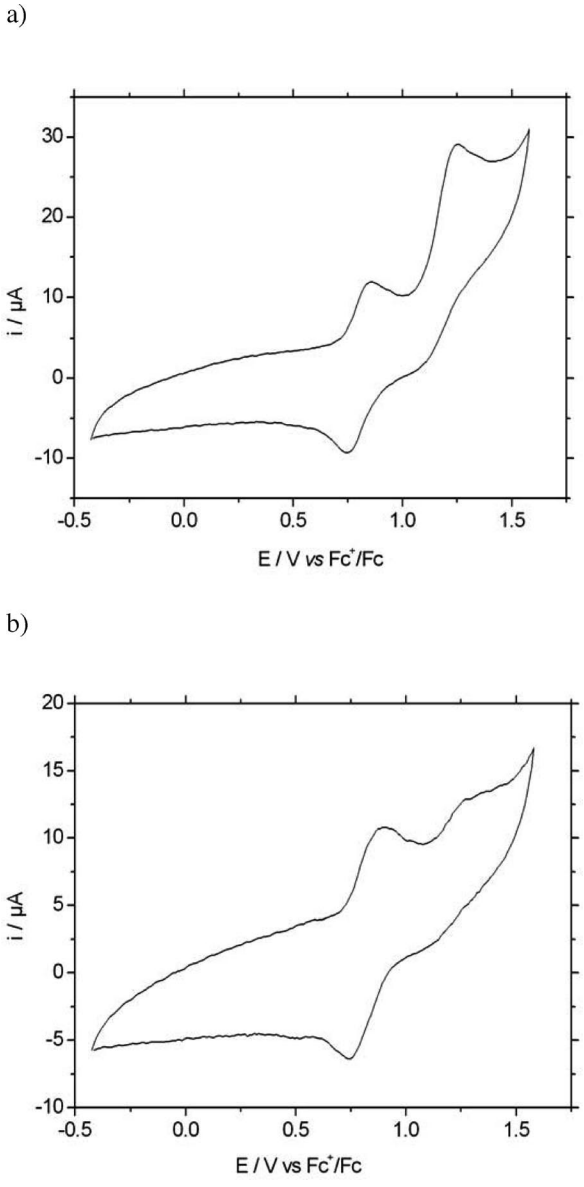

Figure 2. Cyclic voltammetry at a glassy carbon disk (CH_3CN/Bu_4NPF_6 0.1 mol L^{-1}; v = 100 mV.s^{-1}) of millimolar solutions of two different samples of $[Ni_2\mathbf{L^2}]^{4+}$ (a) a mixture of type III and type V stereoisomers (b) type III isomer as the major component.

Table 4. $E^{ox}_{1/2}$ values (in V vs. Fc^+/Fc) of relevant nickel cyclam complexes according to their stereochemistry; quasi-reversibility criterion $i_{pa}/i_{pc} \approx 1$.

Complex	Type I	Type III	Type V
$[Ni_2\mathbf{L^2}]^{4+}$[a]		0.80 (ΔE_p = 120 mV)	1.16 (ΔE_p = 120 mV)
$[Ni_2\mathbf{L^4}]^{4+}$[a]		0.80 (ΔE_p = 100 mV)	1.16 (ΔE_p = 100 mV)
$[Ni_2\mathbf{L^6}]^{4+}$[b]		0.84 (E^{ox}_p irrev.)	1.03 (ΔE_p = 100 mV)
			1.18 (ΔE_p = 100 mV)
$[Ni\mathbf{L^8}]^{2+}$[c]	0.68 (ΔE_p = 90 mV)		1.01 (ΔE_p = 100 mV)
$[Ni\mathbf{L^9}]^{2+}$[c]		0.80 (ΔE_p = 90 mV)	

[a] This work. [b] Ref.[10]. [c] Ref.[26].

azine bismacrocyclic systems, EPR analyses were carried out with the copper analogues $[Cu_2\mathbf{L^{1,2}}]^{4+}$.

EPR Studies of the Bismacrocyclic Complexes

The EPR spectra of the $[Cu_2\mathbf{L^{1,2}}]^{4+}$ complexes were recorded in dmf solution at 150 K (Figure 3, Figure 4). The X-band EPR spectrum of frozen $[Cu_2\mathbf{L^1}]^{4+}$ solution exhibits a strong absorption at approximately 3200 G, attributable to the allowed transitions $\Delta M_S = 1$ (Figure 3a). This spectrum is similar to the one recorded prior to the potentiometric study in frozen aqueous solution with $C_L/C_M < 1$ (see Supporting Information). The recrystallisation of $[Cu_2\mathbf{L^1}]^{4+}$ was then performed and yielded single crystals of $[Cu_2\mathbf{L^1}]^{4+}$, for which the dinuclear structure was confirmed (Figure 1). The EPR spectrum of $[Cu_2\mathbf{L^1}]^{4+}$ single crystals in frozen dmf solution exhibits a strong absorption at approximately 3200 G, and the hyperfine signal consists of four equidistant lines (Figure 3b). The comparison of the EPR spectra of $[Cu_2\mathbf{L^1}]^{4+}$ before and after crystallisation seems to indicate that, in the first spectrum, the complex exists in two isomeric forms (since the purity of the sample as checked by conventional methods is satisfactory).

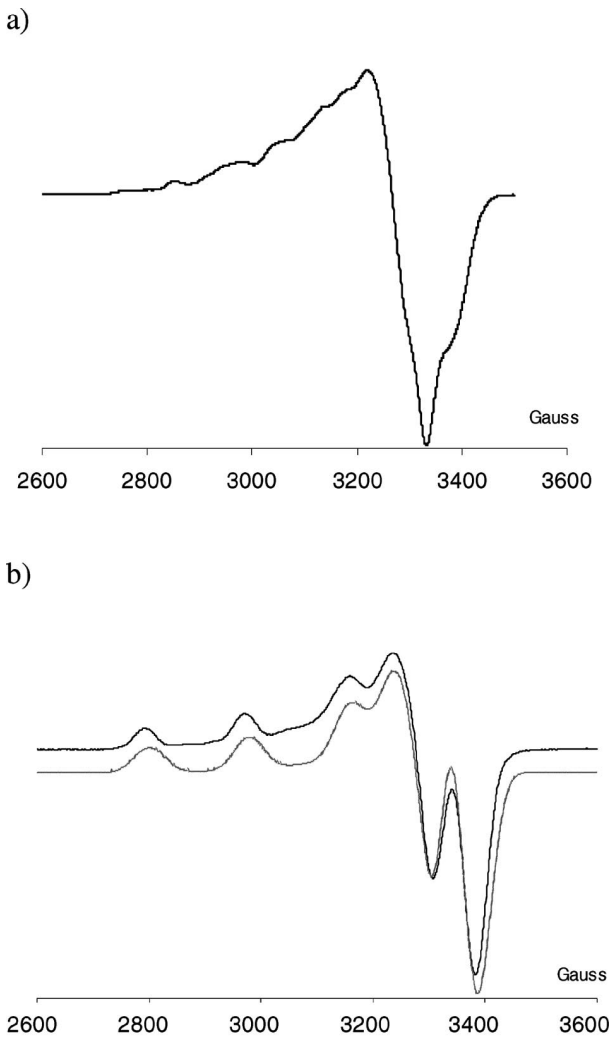

Figure 3. (a) EPR spectra for $[Cu_2\mathbf{L^1}]^{4+}$ (a) before and (b) after recrystallisation [dmf (150 K)]. The dotted lines correspond to the simulated spectrum.

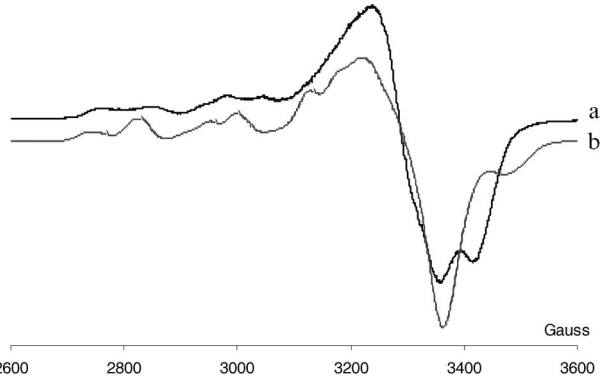

Figure 4. (a) Experimental [dmf (150K)] and (b) calculated EPR spectra for $[Cu_2\mathbf{L^2}]^{4+}$.

The EPR parameters for the crystallised $[Cu_2\mathbf{L^1}]^{4+}$ complex can then be obtained by simulation. The X-Sophe simulation software[27] allows us to construct the molecular Hamiltonian to obtain the spin parameters for the $[Cu_2\mathbf{L^1}]^{4+}$ single crystals. For that, the spin Hamiltonian is taken as

$$\mathbf{H} = \mu_B B\mathbf{g}_A S_A + I_A\mathbf{A}_A S_A + \mu_B B\mathbf{g}_B S_B + I_B\mathbf{A}_B S_B + \mathbf{J}_{AB} S_A S_B + S_A\mathbf{D}S_B$$

where μ_B is the Bohr magneton, $\mathbf{g}_A$, $\mathbf{g}_B$, $\mathbf{A}_A$, $\mathbf{A}_B$ correspond to the individual site **g** and **A** tensors, S_A and S_B are spins on the two copper centres ($S_A = S_B = 1/2$), $\mathbf{J}_{AB}$ accounts for the isotropic exchange interaction and **D** is the zero-field-splitting tensor. For $[Cu_2\mathbf{L^1}]^{4+}$ the overall structure is centrosymmetric. In this condition, the **D** term is null.[28] The spin Hamiltonian parameters of this complex are computed according to Comba's procedure[29] on the basis of the known parameters of the relevant mononuclear complex $[Cu\mathbf{L^7}]^{2+}$ ($g_\parallel = 2.192$, $g_\perp = 2.045$, $A_\parallel = 175 \times 10^{-4}$ cm^{-1} and $A_\perp = 15.6 \times 10^{-4}$ cm^{-1}).[18] This is supported by the fact that the individual site tensors in the dinuclear complex are not expected to deviate much from those of the mononuclear complex.[31] For the perturbation treatment, it is necessary to take into account the complex geometry, that is to say, the Cu–Cu distance (r_{AB}), the structural parameters τ, η and ζ describing the orientation of one CuN_4 chromophore relative to the other (Figure 5)[29a] and finally the Euler angles. So, in the first step of the spectrum simulation, the structural parameters from the X-ray structure were used as input data [$r_{AB} = 7$ Å, $\tau = 0°$, $\eta = 0°$ (the two CuN_4 chromophores are parallel), $\xi = 30°$]. The magnetic exchange constant between metal ions is weak and taken to be equal to -25×10^{-4} cm^{-1}, which is the magnitude of **J** for this type of complexes.[29a] After optimisation, the resulting computed spectrum (Figure 3b dotted lines) gives an acceptable fit with the experimental spectrum, and the simulated EPR parameters are $g_\parallel = 2.195$, $g_\perp = 2.051$ (Table 5).

These values ($g_{\parallel} > g_{\perp}$) are typical of axially symmetric d^9 copper complexes with a $d_{x^2-y^2}$ ground state.[30] The hyperfine coupling constant for the spectrum of $[Cu_2\mathbf{L^1}]^{4+}$ single crystals is equal to 180×10^{-4} cm^{-1}. This result supports the previously formulated assumptions i.e. **D** equal to zero and a very weak **J** amplitude. This signifies that in this complex, spin delocalisation towards the pyrazine nitrogen atoms is poor. Magnetic interactions through the bridging pyrazine ligand are often described as weak.[11] Furthermore, the direction of magnetic copper orbitals towards the bridging pyrazine ligand is important, since an unfavourable overlap of the corresponding orbitals prevents the development of such interactions. The $[Cu_2\mathbf{L^1}]^{4+}$ structure indicates that the $d_{x^2-y^2}$ copper orbitals (the *x* and *y* axes are roughly defined by the Cu–N macrocyclic bonds) are orthogonal to the pyrazine nitrogen lone pairs located in axial positions. Therefore the overlap is null, and the two magnetic centres behave almost independently, leading in the parallel region to a signal similar to that of mononuclear complexes.[18]

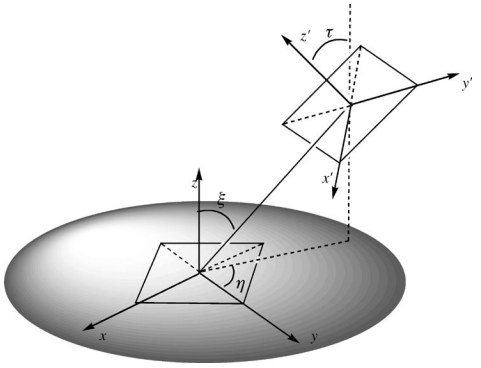

Figure 5. Definition of the structural parameters used in the spin Hamiltonian (ref.[29a]) for the simulation of the EPR spectrum of $[Cu_2\mathbf{L^{1,2}}]^{4+}$.

Table 5. EPR parameters of $[Cu_2\mathbf{L^{1,2}}]^{4+}$ complexes in dmf solution at 150 K.

	$g_{\parallel}$	$g_{\perp}$	$A_{\parallel}$ /10^{-4} cm^{-1}
$[Cu_2\mathbf{L^1}]^{4+}$[a]	2.195	2.051	178.5
$[Cu_2\mathbf{L^2}]^{4+}$	2.195	2.045	180

[a] Single crystals.

For $[Cu_2\mathbf{L^2}]^{4+}$, the hyperfine system can be interpreted as consisting of four equidistant lines, the shoulders being observed for each line of the system (Figure 4a). The global signal shape can be explained on the basis of the partial knowledge of the copper coordination sphere in this complex (Figure S6). Since the structure seems to be centrosymmetric, four lines are expected in the parallel region of the EPR spectrum. The signal splitting may then result from a distortion of the complex geometry as described previously for relevant spiro complexes.[6b] If the two macrocyclic CuN_4 planes are tilted towards each other and are orthogonal to the pyrazine bridge, this may generate a local anisotropy that differentiates the two Cu^{II} centres.

As it has been shown in similar cases, the origin of this interaction is purely dipolar.[6b,31] To test this hypothesis, a spectrum simulation similar to the one previously performed for $[Cu_2\mathbf{L^1}]^{4+}$ was undertaken. In the first step of the simulation, the structural parameters of the partial $[Cu_2\mathbf{L^2}]^{4+}$ structure were used as input data [r_{AB} = 7.2 Å, τ = 0°, η = 15° (the two CuN_4 chromophores are slightly tilted), ξ = 45° – see Figure S6]. The spin Hamiltonian parameters used in the first step are the parameters determined for the type III $[Cu\mathbf{L^8}]^{2+}$ complex ($g_{\parallel}$ = 2.197, $g_{\perp}$ = 2.045, $A_{\parallel}$ = 188.7×10^{-4} cm^{-1} and $A_{\perp}$ = 22.5×10^{-4} cm^{-1}).[18] An exchange constant of $J = -25 \times 10^{-4}$ cm^{-1} was firstly used for the calculation. Unfortunately, these data did not yield an acceptable fit between the simulated and experimental spectrum. A single-point calculation was then attempted by modifying some parameters of the model (r_{AB} = 7.2 Å, τ = 0°, η = 15°, ξ = 70°, $J = -130 \times 10^{-4}$ cm^{-1}). The resulting calculated spectrum fits better with the experimental one (Figure 4b). The corresponding EPR parameters are listed in Table 5. This incomplete optimisation seems, however, to indicate that the formulated hypothesis, i.e. that the signal splitting is a consequence of the complex geometry with a local anisotropy that differentiates the two copper centres, seems reasonable.

Conclusions

Dinuclear Cu^{II} and Ni^{II} complexes based on bis(cyclen) ($\mathbf{L^1}$) and bis(cyclam) ($\mathbf{L^2}$) ligands have been studied. X-ray analysis of the $[Cu_2\mathbf{L^1}]^{4+}$, $[Cu_2\mathbf{L^2}]^{4+}$and $[Ni_2\mathbf{L^1}]^{4+}$ complexes have shown that the pyrazine nitrogen atom coordinates the two metal ions. This coordination remains in solution. Furthermore, configurational isomers can be detected in solution for $[Ni_2\mathbf{L^2}]^{4+}$ by cyclic voltammetry. Potentiometric investigations have indicated that the coordination of nitrogen pyrazine atoms to the metal centres does not affect the stability of the complexes. As indicated by the X-ray structure, the coordination of the pyrazine nitrogen atoms leads to the shortening of the intermetallic copper–copper distance in comparison with the corresponding *para*-xylyl ligands. The evaluation of the possible intermetallic interactions was then investigated by electrochemical and EPR measurements. These experiments have shown that the pyrazine bridge is a relatively inefficient exchange bridging ligand between the two coordinated metal centres in these complexes. The first reason lies in the fact that this ligand is known to give a poor superexchange pathway. The second reason results from the apical position of the pyrazine bridge in the copper coordination sphere, which imposes an orthogonality on the copper(II) magnetic orbitals and the lone pairs of the pyrazine nitrogen atoms. This leads to a peculiar EPR fingerprint of four lines in the parallel region for these dinuclear complexes. These lines may be further be divided in two if a fortuitous local anisotropy differentiates the two metal centres without necessarily creating a superexchange pathway.

Experimental Section

The metal salts were purchased from Aldrich. The other reagents were used as highest grade commercially available without further purification.

Synthesis of the Ligands: The ligands **L¹** and **L²** have been synthesised according to the bis(aminal) methodology[12] by alkylation of cyclen–glyoxal and cyclam–glyoxal with 2,5-bis(chloromethyl)-pyrazine (obtained according to ref.[32]). Prior to cyclen–glyoxal and cyclam–glyoxal alkylation, 2,5-bis(chloromethyl)pyrazine (2.2 mmol) and NaI (4.4 mmol) were dissolved in dry acetonitrile (10 mL). After stirring for two hours at room temperature, a white precipitate of NaCl was removed from the solution by filtration. The resulting solution was then added dropwise to a solution of cyclen–glyoxal or cyclam–glyoxal (4 mmol) dissolved in dry acetonitrile (10 mL). The mixture was stirred at room temperature for four days. The precipitate was collected by filtration, washed with acetonitrile and dried in vacuo, giving the bismacrocyclic bis(aminal) compounds **L¹a** and **L²b** (see Scheme S7). These bis(aminal)s (2 mmol) were further deprotected by addition of hydrazine monohydrate (10 mL) at 120 °C for 3 h. After cooling, the resulting precipitate was collected by filtration, washed with ethanol and dried under vacuum to give **L¹** and **L²**.

Ligand L¹: Overall yield: 65%, 0.665 g. ^{1}H NMR (500 MHz, D_2O): 2.56 (t, 8 H, CH_2N), 2.62 (m, 16 H, CH_2N), 2.69 (t, 8 H, CH_2N), 3.79 (s, 4 H, pyrazineCH_2N), 8.59 (s, 2 H, CH_{ar}) ppm. ^{13}C NMR (62.9 MHz, D_2O): δ = 43.8, 44.9, 45.6, 51.3, 57.4(CH_2N), 153.5, 144.6 (5C_{ar}) ppm. $C_{22}H_{44}N_{10}\cdot 3.5H_2O$ (511.72): calcd. C 51.64, H 10.04, N 27.37; found C 51.56, H 9.82, N 27.14.

Ligand L²: Overall yield: 65%, 0.691 g. ^{1}H NMR (500 MHz, D_2O): 1.54 (q, 4 H, CH_2CH$_2$N), 1.70 (q, 4 H, CH_2CH$_2$N), 2.43 (m, 8 H, CH_2N), 2.50 (m, 12 H, CH_2N), 2.57 (t, 4 H, CH_2N), 2.63 (t, 8 H), 3.70 (s, 4 H, pyrazineCH_2N), 8.57 (s, 2 H, CH_{ar}) ppm. ^{13}C NMR (62.9 MHz, D_2O): δ = 25.3, 27.3 (CH$_2$CH$_2$N), 46.0, 46.8, 47.1, 47.8, 48.1, 48.8, 54.1, 54.2, 56.5 (CH$_2$N), 153.6, 144.2 (C_{ar}) ppm. $C_{26}H_{52}N_{10}\cdot 1.5H_2O$ (531.79): calcd. C 58.72, H 10.42, N 26.34; found C 58.94, H 10.41, N 26.20.

Synthesis of Copper and Nickel Complexes: The neutral ligands (5.2×10^{-5} mol) were dissolved in methanol (15 mL), and methanol solutions of copper(II) or nickel(II) salts (1.17×10^{-4} mol in 5 mL) were added dropwise. The resulting solutions were heated at reflux for 2 h. The solutions were further concentrated, and addition of diethyl ether allowed precipitation of the complexes. The solids were then collected by filtration and dried under vacuum. Their purity was controlled by mass spectrometry and elemental analysis. The solids were further dissolved in acetonitrile, and the diffusion of a diethyl ether solution produced single crystals of $[Cu_2\mathbf{L^1}]^{4+}$, $[Cu_2\mathbf{L^2}]^{4+}$ and $[Ni_2\mathbf{L^1}(CH_3CN)_2]^{4+}$. It should be noted that for $[Ni_2\mathbf{L^1}(CH_3CN)_2]^{4+}$ two different samples were collected for which the mass spectrum and the elemental analysis were rigorously the same.

CAUTION: Perchlorate-containing complexes are potentially explosive and appropriate precautions should be in place for their preparation, handling and storage.

$[Cu_2\mathbf{L^1}](ClO_4)_4$: Blue solid, 60%, 0.0304 g. $C_{22}H_{44}N_{10}Cu_2Cl_4O_{16}$ (973.54): calcd. C 27.14, H 4.55, N 14.13; found C 27.09, H 4.49, N 14.20. ESI-MS: calcd. for $[Cu_2(C_{22}H_{44}N_{10})(ClO_4)_3]^+$ 871.1; found 871.0.

$[Cu_2\mathbf{L^2}](ClO_4)_4\cdot 0.5H_2O$: Blue solid, 53%, 0.0286 g. $C_{26}H_{52}N_{10}Cl_4Cu_2O_{16}\cdot 0.5H_2O$ (1038.66): calcd. C 30.06, H 5.14, N 13.48; found C 30.03, H 5.02, N 13.21. ESI-MS: calcd. for $[Cu_2(C_{26}H_{52}N_{10})(ClO_4)_3]^+$ 927.1; found 927.0.

$[Ni_2\mathbf{L^1}](ClO_4)_4\cdot H_2O$: Yellow solid, 72%, 0.0362 g. $C_{22}H_{44}N_{10}Cl_4Ni_2O_{16}\cdot 0.25H_2O$ (968.34): calcd. C 26.91, H 4.72, N 14.26; found C 27.10, H 5.08, N 14.16. ESI-MS: calcd. for $[Ni_2(C_{22}H_{44}N_{10})(ClO_4)_3]^+$ 861.09; found 861.09.

$[Ni_2\mathbf{L^2}](ClO_4)_4\cdot 2CH_3OH$: Yellow solid, 68%, 0.0383 g. $C_{26}H_{52}N_{10}Cl_4Ni_2O_{16}\cdot 2CH_3OH$ (1084.03): calcd. C 30.91, H 5.48, N 2.39; found C 31.01, H 5.54, N 12.92. ESI-MS: calcd. for $[Ni_2(C_{26}H_{52}N_{10})(ClO_4)_3]^+$ 917.15; found 917.20.

Potentiometric Measurements

Potentiometric titrations were carried out with an automatic titrator composed of a microprocessor burette Metrohm dosimat 665 and a pHmeter Metrohm 713 connected to a computer. The combined Type "U" glass electrode Metrohm used had a very low alkaline error. The titration procedure was fully automated. All measurements were performed within a thermoregulated cell at 20.0 ± 0.1 °C under an argon stream to avoid the dissolution of carbon dioxide. The ionic strength was adjusted to 1 with potassium nitrate. The ionic product of water was determined under these conditions (pK_w = 13.93). Solutions of ligand (1×10^{-3} to 2×10^{-3} mol L^{-1}) were titrated with a KOH solution (0.1 mol L^{-1}). For the complexation studies, several ligand/copper nitrate mixtures (ligand/metal ratio in the range 0.5–2 for a ligand concentration of 10^{-3}mol L^{-1} in the measurement cell) at acidic initial pH were stored under argon in a thermoregulated enclosure at 40 °C for four, six and eight weeks. Before titration with a KOH solution (0.1 mol L^{-1}), these solutions were allowed to reach the equilibrium temperature (25 °C) for 48 h.

The protometric data were processed by using the PROTAF program[13] to obtain the best fit chemical model and refined overall constants β_{mlh}.

$$m\mathrm{M} + l\mathrm{L} + h\mathrm{H}^+ \rightleftharpoons \mathrm{M}_m\mathrm{L}_l\mathrm{H}_h \qquad \beta_{mlh} = \frac{[M_m L_l H_h]}{[M]^m[L]^l[H^+]^h}$$

The stepwise protonation constants (K_{0lh}) related to equilibrium (1) are defined by equation (2) and were deduced from the refined β_{0lh} values given by relation (3):

$$\mathrm{LH}_{h-1}^{(h-1)+} + \mathrm{H}^+ \overset{K_{0lh}}{\rightleftharpoons} \mathrm{LH}_h^{h+} \quad (1)$$

$$K_{0lh} = \frac{[LH_h^{h+}]}{[LH_{h-1}^{(h-1)+}][H^+]} \quad (2)$$

$$\beta_{0lh} = \prod_{i=1}^{h} K_{0li} \quad (3)$$

Each titration made use of at least 15 points per neutralisation curve, and titrations were repeated until a satisfactory agreement was reached. A minimum of ten curves were used for the determination of the **L¹** and **L²** protonation constants, while for the determination of the complexation constants, six curves were used for each [L]/[M] ratio. The confidence intervals based on the standard deviation obtained for the different protonation constants and overall complexation constants are given in Figure S1.

The potentiometric data used for the determination of the complexation constants of the mononuclear complexes towards Cu^{II} corresponded to the ratios C_L/C_M = 1.7 and 2. Under these condi-

tions, either the EPR or the mass spectra of the corresponding solutions recorded in water at different pH indicated the sole presence of the mononuclear complexes. The calculations were then performed without considering the formation of the dinuclear species. The potentiometric data used for the determination of the complexation constants of the dinuclear complexes corresponded to the ratio $C_L/C_M = 0.58$. Under these conditions, either the EPR or the mass spectra of the corresponding solutions recorded in water at different pH indicated the sole presence of the dinuclear complexes. The calculations were then performed without considering the formation of the mononuclear species.

Spectroscopic Measurements

Electronic spectra in aqueous or acetonitrile solutions (10^{-3} mol L^{-1}) were all measured in the 300–900 nm range with a Lambda 6 Perkin–Elmer spectrophotometer.

EPR spectra were recorded with a Bruker ESP 300e spectrometer (X-band) equipped with a Bruker E035M gaussmeter and a HP 5350B microwave frequency counter. Samples were prepared at a concentration of 5 mmol L^{-1} in dmf frozen solutions (150 K – Bruker ER4111VT variable temperature unit). The best resolution was obtained at $T = 150$ K by using the modulation amplitude 2.66 G for $[Cu_2\mathbf{L^1}]^{4+}$ 0.596 G for $[Cu_2\mathbf{L^2}]^{4+}$, time constant 655.36 ms, conventional time 327.68 ms and sweep time 335.54 ms. The simulation of the high-field EPR spectra were performed by using XSophe software version 1.1.4 for Mandriva 2006 x86_64 developed by the centre for Magnetic Resonance and the Department of Mathematics of the University of Queensland, Brisbane, Australia, for Bruker Biospin GmbH.[27] The software uses a linewidth model with an angular dependence of g and a Simplex optimisation method with the copper element in a natural abundance (for $[Cu_2\mathbf{L^1}]^{4+}$: linewidth in the parallel region = 23.7×10^{-4} cm^{-1}, linewidth in the perpendicular region = 19.8×10^{-4} cm^{-1}; for $[Cu_2\mathbf{L^2}]^{4+}$: linewidth in the parallel region = 30.0×10^{-4} cm^{-1}, linewidth in the perpendicular region = 30.0×10^{-4} cm^{-1}).

Electrochemical Measurements: Voltammetric data were recorded with an "Autolab with PGSTAT12" potentiostat (ECO Chemie) associated to a conventional three-electrode electrochemical cell, the working electrode being a glassy carbon disk, and a platinum plate being used as a counterelectrode and a silver electrode in acetonitrile separated from the complex solution was used as a pseudoreference. The potential of the pseudoreference was measured vs. the ferricinium/ferrocene couple. Concentrations of the complexes were always close to 10^{-3} mol L^{-1} and in acetonitrile tetrabutylammonium hexafluorophosphate (10^{-1} mol L^{-1}) was used as the supporting electrolyte.

Crystal Structure Determination

The crystal data were collected at 173 K with a Kappa CCD diffractometer by using monochromated Mo-K_α radiation (λ = 0.71073 Å). The structure was solved by direct methods. After refinement of the non-hydrogen atoms, difference-Fourier maps revealed maxima of residual electron density close to positions expected for hydrogen atoms. Hydrogen atoms were introduced as fixed contributors at calculated positions [C–H 0.95 Å, B(H) 1.3 $B_{eqv.}$]. Final difference maps revealed no significant maxima. All calculations were performed by using the Nonius OpenMoleN package.[33] Neutral atom scattering factor coefficients and anomalous dispersion coefficients were taken from a standard source. Molecular formula: $C_{26}H_{50}N_{12}B_4F_{16}Cu_2$, M_r = 1005.1 g mol^{-1}, orthorhombic, *Pbca* (Nr 61), a = 11.574(5) Å, b = 15.620(5) Å, c = 22.322(5) Å, V = 4036(2) Å^3, Z = 4, D_{calc} = 1.654 g cm^{-3}, μ = 1.167 mm^{-1}, $F_{(ooo)}$ = 2048, T = 173 K. A total of 53662 reflections were collected; there are 4604 independent reflections. Final R values are: R = 0.052 for 3150 observed reflections, R(all data) = 0.087, wR = 0.126, S = 1.03, largest difference peaks/holes: 0.819/–0.687 e Å^{-3}.

CCDC-677258 contains the supplementary crystallographic data for this paper. These data can be obtained free of charge from The Cambridge Crystallographic Data Centre via www.ccdc.cam.ac.uk/data_request/cif.

For $[Ni_2\mathbf{L^1}]^{4+}$ and $[Cu_2\mathbf{L^2}]^{4+}$ we were unable to obtain high-quality single crystals, but the data, although poor, allowed a qualitative description of the structures (see Figures S5 and S6).

Supporting Information (see footnote on the first page of this article): potentiometric titrations curves (Figure S1), distribution speciation diagrams for $\{\mathbf{L^1} - Cu^{II}\}$ and $\{\mathbf{L^2} - Cu^{II}\}$ systems (Figures S2 and S3), the comparison of $\mathbf{L^1}$ and $\mathbf{L^2}$ affinities towards Cu^{II} by comparison with relevant ligands (Figure S4), the Schakal diagram of $[Ni_2\mathbf{L^1}(CH_3CN)_2]^{4+}$ (Figure S5) and the coordination polyhedron of Cu^{II} in $[Cu_2\mathbf{L^2}]^{4+}$ (Figure S6). Finally, the synthesis of $\mathbf{L^1}$ and $\mathbf{L^2}$ is reported in Scheme S7.

Acknowledgments

We thank Dr. G. Blondin (Laboratoire Physico-Chimie des Métaux en Biologie, CEA – GRENOBLE, France) for helpful discussions.

[1] a) R. Delgado, V. Félix, L. M. P. Lima, D. W. Price, *Dalton Trans.* **2007**, 2734–2745; b) A. Bencini, A. Bianchi, P. Paoletti, *Coord. Chem. Rev.* **1992**, *120*, 51–85; c) . A. Bianchi, M. Micheloni, P. Paoletti, *Coord. Chem. Rev.* **1991**, *110*, 17–113.

[2] a) R. Reichenbach-Klinke, B. König, *J. Chem. Soc., Dalton Trans.* **2002**, 121–130; b) J. D. Chartres, L. F. Lindoy, G. V. Mechan, *Coord. Chem. Rev.* **2001**, *216–217*, 219–286; c) A. McAuley, S. Subramanian, *Coord. Chem. Rev.* **2000**, *200–202*, 75–103; d) T. A. Kaden, *Coord. Chem. Rev.* **1999**, *190–192*, 371–389; e) G. De Santis, L. Fabbrizzi, M. Lichelli, P. Pallavicini, *Coord. Chem. Rev.* **1992**, *120*, 237–257.

[3] a) S. Develay, R. Tripier, M. Le Baccon, V. Patinec, G. Serratrice, H. Handel, *Dalton Trans.* **2006**, 3418–3426; b) M. Lachkar, R. Guilard, A. Atmani, A. De Cian, J. Fischer, R. Weiss, *Inorg. Chem.* **1998**, *37*, 1575–1584.

[4] a) Y. Dong, L. F. Lindoy, P. Turner, G. Wei, *Dalton Trans.* **2004**, 1264–1270; b) C. Bazzicalupi, A. Bencini, E. Berni, C. Giorgi, S. Maoggi, B. Valtancoli, *Dalton Trans.* **2003**, 3574–3580; c) A. Bencini, E. Berni, A. Bianchi, C. Giorgi, B. Valtancoli, D. K. Chand, H. J. Schneider, *Dalton Trans.* **2003**, 793–800.

[5] a) S. Aoki, E. Kimura, *Chem. Rev.* **2004**, *104*, 769–787; b) S. Aoki, E. Kimura, *J. Am. Chem. Soc.* **2000**, *122*, 4542–4548; c) E. Kimura, M. Kituchi, H. Kitamura, T. Koike, *Chem. Eur. J.* **1999**, *5*, 3113–3123.

[6] a) P. Comba, Y. D. Lampeka, L. Lötzbeyer, A. I. Prikhod′ko, *Eur. J. Inorg. Chem.* **2003**, 34–37; b) A. McAuley, S. Subramanian, M. J. Zawarotko, K. Biradha, *Inorg. Chem.* **1999**, *38*, 5078–5085; c) A. McAuley, S. Subramanian, *Inorg. Chem.* **1997**, *36*, 5376–5383.

[7] P. J. Hay, J. C. Thibeault, R. Hoffmann, *J. Am. Chem. Soc.* **1975**, *97*, 4884–4899.

[8] a) M. Ciampolini, L. Fabbrizzi, A. Perotti, A. Poggi, B. Seghi, F. Zanobini, *Inorg. Chem.* **1987**, *26*, 3527–3533; b) L. Fabbrizzi, L. Montagna, A. Poggi, T. A. Kaden, L. Siegfried, *J. Chem. Soc., Dalton Trans.* **1987**, 2631–2634; c) R. Schneider, A. Riesen, T. A. Kaden, *Helv. Chim. Acta* **1986**, *69*, 53–61; d) L. Fabbrizzi, L. Montagna, A. Poggi, T. A. Kaden, L. Siegfried, *Inorg. Chem.* **1986**, *25*, 2671–2672; e) L. Fabbrizzi, F. Forlini, A. Perotti, B. Seghi, *Inorg. Chem.* **1984**, *23*, 807–813.

[9] a) C. Bucher, J. C. Moutet, J. Pécaut, G. Royal, E. Saint-Aman, F. Thomas, *Inorg. Chem.* **2004**, *43*, 3777–3779; b) C. Bucher,

J. C. Moutet, J. Pécaut, G. Royal, E. Saint-Aman, F. Thomas, S. Torelli, M. Ungureanu, *Inorg. Chem.* **2003**, *42*, 2242–2252; c) D. T. Pierce, T. L. Hatfield, E. J. Billo, Y. Ping, *Inorg. Chem.* **1997**, *36*, 2950–2955.
[10] S. El Ghachtouli, C. Cadiou, I. Déchamps-Olivier, F. Chuburu, M. Aplincourt, V. Turcry, M. Le Baccon, H. Handel, *Eur. J. Inorg. Chem.* **2005**, 2658–2668.
[11] a) H. Oshio, U. Nagashima, *Inorg. Chem.* **1990**, *29*, 3321–3325; b) M. Graf, H. Stoeckli-Evans, A. Escuer, R. Vicente, *Inorg. Chim. Acta* **1997**, *257*, 89–97; c) D. S. Cati, J. Ribas, J. Ribas-Arino, H. Stoeckli-Evans, *Inorg. Chem.* **2004**, *43*, 1021–1030; d) J. Klingele, B. Moubaraki, K. S. Murray, J. F. S. Brooker, *Eur. J. Inorg. Chem.* **2005**, 1530–1541; e) J. Klingele, J. F. Boas, J. R. Pilbrow, B. Moubaraki, K. S. Murray, K. J. Berry, K. A. Hunter, G. B. Jameson, P. D. W. Boyd, S. Brooker, *Dalton Trans.* **2007**, 633–645.
[12] M. Le Baccon, F. Chuburu, L. Toupet, H. Handel, M. Soibinet, I. Déchamps-Olivier, J. P. Barbier, M. Aplincourt, *New J. Chem.* **2001**, *25*, 1168–1174.
[13] a) R. Fournaise, C. Petitfaux, *Analusis* **1990**, *18*, 242–249; b) R. Fournaise, C. Petitfaux, *Talanta* **1987**, *34*, 385–395.
[14] M. Soibinet, I. Déchamps-Olivier, E. Guillon, J. P. Barbier, M. Aplincourt, F. Chuburu, M. Le Baccon, H. Handel, *Eur. J. Inorg. Chem.* **2003**, 1984–1994.
[15] S. Develay, R. Tripier, M. Le Baccon, V. Patinec, G. Serratrice, H. Handel, *Dalton Trans.* **2005**, 3016–3024.
[16] a) M. Arca, A. Bencini, E. Berni, C. Caltagirone, F. A. Devillanova, F. Isaia, A. Garau, C. Giorgi, V. Lippolis, A. Pera, L. Tei, B. Valtancoli, *Inorg. Chem.* **2003**, *42*, 6929–6939; b) K. J. Powell, Academic software, Mini SC Database, version 5.3, **1999**; c) J. Malik, R. Shepered, *J. Inorg. Nucl. Chem.* **1972**, *34*, 3203–3207.
[17] P. Antunes, R. Delgado, M. G. B. Drew, V. Félix, H. Maecke, *Inorg. Chem.* **2007**, *46*, 3144–3153.
[18] S. El Ghachtouli, C. Cadiou, I. Déchamps-Olivier, F. Chuburu, M. Aplincourt, T. Roisnel, *Eur. J. Inorg. Chem.* **2006**, 3472–3481.
[19] a) A. E. Goeta, J. A. K. Howard, D. Maffeo, H. Puschmann, J. A. Gareth Williams, D. S. Yufit, *J. Chem. Soc., Dalton Trans.* **2000**, 1873–1880; b) V. J. Thorn, C. C. Fox, J. C. A. Boeynes, R. D. Hancock, *J. Am. Chem. Soc.* **1984**, *106*, 3198–3207.
[20] A. W. Addison, T. N. Rao, J. Reedijk, J. van Rijn, G. C. Verschoot, *J. Chem. Soc., Dalton Trans.* **1984**, 1349–1356.
[21] S. Brandès, C. Gros, F. Denat, P. Pullumbi, R. Guilard, *Bull. Soc. Chim. Fr.* **1996**, *133*, 65–73.
[22] B. Bosnich, C. K. Poon, M. L. Tobe, *Inorg. Chem.* **1965**, *4*, 1102–1108.
[23] a) A. Buttafava, L. Fabbrizzi, A. Perotti, A. Poggi, G. Poli, B. Seghi, *Inorg. Chem.* **1986**, *25*, 1456–1461; b) A. Bencini, L. Fabbrizzi, A. Poggi, *Inorg. Chem.* **1981**, *20*, 2544–2549.
[24] a) L. Fabbrizzi, *Comments Inorg. Chem.* **1985**, *4*, 33–54; b) C. Bisi Castellani, M. Licchelli, A. Perotti, A. Poggi, *J. Chem. Soc., Chem. Commun.* **1984**, 806–808; c) F. V. Lovecchio, E. S. Gore, D. H. Busch, *J. Am. Chem. Soc.* **1974**, *96*, 3109–3118.
[25] M. Ciampolini, L. Fabbrizzi, M. Licchelli, A. Perotti, F. Pezzini, A. Poggi, *Inorg. Chem.* **1986**, *25*, 4131–4135.
[26] S. El Ghachtouli, C. Cadiou, I. Déchamps-Olivier, F. Chuburu, M. Aplincourt, V. Patinec, M. Le Baccon, H. Handel, T. Roisnel, *New J. Chem.* **2006**, *30*, 392–398.
[27] a) M. Griffin, A. Muys, C. Noble, D. Wang, C. Eldershaw, K. E. Gates, K. Burrage, G. R. Hanson, *Mol. Phys. Rep.* **1999**, *26*, 60–84; b) G. R. Hanson, K. E. Gates, C. J. Noble, M. Griffin, A. Mitchell, S. Benson, *J. Inorg. Biochem.* **2004**, *98*, 903–916.
[28] J. R. Pilbrow, *Transition Ion Electron Paramagnetic Resonance*, Oxford University Press, New York, **1991**, p. 334.
[29] a) P. Comba, Y. D. Lampeka, A. I. Prikhod′ko, G. Rajaraman, *Inorg. Chem.* **2006**, *45*, 3632–3638; b) G. Cavigliasso, P. Comba, R. Stranger, *Inorg. Chem.* **2004**, *43*, 6734–6744.
[30] B. J. Hathaway, A. A. G. Tomlinson, *Coord. Chem. Rev.* **1970**, *5*, 1–43.
[31] T. D. Smith, J. R. Pilbrow, *Coord. Chem. Rev.* **1974**, *13*, 173–278.
[32] U. Eiermann, C. Krieger, F. A. Neugebauer, H. A. Staab, *Chem. Ber.* **1990**, *123*, 523–533.
[33] OpenMoleN, *Interactive Structure Solutions*, Nonius B. V. Delft, The Netherlands, **1997**.
[34] R. D. Hancock, R. J. Motekaitis, J. Mashishi, I. Cukrowski, J. H. Reibenspies, A. E. Martell, *J. Chem. Soc. Perkin Trans. 2* **1996**, 1925–1929.

Received: February 8, 2008
Published Online: September 12, 2008

